PHYSICAL REVIEW B **83**, 174411 (2011)

Integer spin-chain antiferromagnetism of the 4*d* oxide $CaRuO_3$ with post-perovskite structure

Y. Shirako,[1,2,*] H. Satsukawa,[3] X. X. Wang,[2,4] J. J. Li,[2,4] Y. F. Guo,[5] M. Arai,[6] K. Yamaura,[2,4,7] M. Yoshida,[1] H. Kojitani,[1] T. Katsumata,[1] Y. Inaguma,[1] K. Hiraki,[3] T. Takahashi,[3] and M. Akaogi[1]

[1]*Department of Chemistry, Gakushuin University, 1-5-1 Mejiro, Toshima-ku, Tokyo 171-8588, Japan*

[2]*Superconducting Materials Center, National Institute for Materials Science, 1-1 Namiki, Tsukuba, Ibaraki 305-0044, Japan*

[3]*Department of Physics, Gakushuin University, 1-5-1 Mejiro, Toshima-ku, Tokyo 171-8588, Japan*

[4]*Department of Chemistry, Graduate School of Science, Hokkaido University, Sapporo, Hokkaido 060-0810, Japan*

[5]*International Center for Materials Nanoarchitectonics (MANA), National Institute for Materials Science, 1-1 Namiki, Tsukuba, Ibaraki 305-0044, Japan*

[6]*Computational Materials Science Center, National Institute for Materials Science, 1-1 Namiki, Tsukuba, Ibaraki 305-0044, Japan*

[7]*JST, Transformative Research-Project on Iron Pnictides (TRIP), 1-1 Namiki, Tsukuba, Ibaraki 305-0044, Japan*

(Received 2 March 2011; revised manuscript received 4 April 2011; published 5 May 2011; corrected 17 May 2011)

A quasi-one-dimensional magnetism was discovered in the post-perovskite $CaRuO_3$ (Ru^{4+}: $4d^4$, *Cmcm*), which is isocompositional with the perovskite $CaRuO_3$ (*Pbnm*). An antiferromagnetic (AFM) spin-chain function with $-J/k_B = 350$ K reproduces the experimental curve of the magnetic susceptibility vs temperature well, suggesting long-range AFM correlations. The anisotropic magnetism is probably owed to the d_{yz}-$2p_\pi$-d_{zx} and d_{zx}-$2p_\pi$-d_{yz} superexchange bonds along the *a* axis. The Sommerfeld coefficient of the specific heat is fairly small, 0.16(2) mJ mol^{-1} K^{-2}, indicating that the magnetism reflects the localized nature of the 4*d* electrons. This is an observation of an integer ($S = 1$) spin-chain AFM in the 4*d* electron system.

DOI: 10.1103/PhysRevB.83.174411 PACS number(s): 74.70.Pq, 73.90.+f

I. INTRODUCTION

A high-pressure dense phase of $CaRuO_3$ was recently created by high-pressure and high-temperature experiments, and it was successfully quenched to ambient conditions.[1,2] The crystal structure at ambient conditions was identified to be of the post-perovskite (PPv) type, which is entirely different from the perovskite (Pv) structure of the regularly synthesized $CaRuO_3$.[1] The newly synthesized phase is 1.7% denser in volume than the Pv $CaRuO_3$.[1] A quick look at the PPv structure (Fig. 1) indicates that it comprises a Ca^{2+} layer and a $RuO_3{}^{2-}$ layer, which alternatively stacks up along the *b* axis [*Cmcm* (Ref. 1)]. The RuO_3 layer consists of RuO_6 octahedra (Ru^{4+}:$4d^4$) connecting to neighbors by sharing common edges and corners along the *a* and *c* axes, respectively. The highly anisotropic structure suggests a very anisotropic electronic state compared with the known Pv $CaRuO_3$. Thus, we decided to study the possible anisotropic properties because, generally, new and valuable correlated properties, such as high-T_c superconductivity induced by metallization via chemical doping or physical squeezing can be expected for such anisotropically correlated materials.

Early studies concluded that $CaRuO_3$ was a paramagnetic metal.[4–6] In the 1990s, however, NMR studies and the development of the theoretical understanding of itinerant electrons revealed that it is a nearly ferromagnetic metal rather than a paramagnetic metal, although it does not show a magnetically long-range order.[7–10] In addition, disorder-induced ferromagnetic behavior was observed in 2001, suggesting that $CaRuO_3$ is indeed in the vicinity of a magnetic critical point between ferromagnetic and paramagnetic states.[11,12] However, by using Mössbauer spectroscopy, a magnetic glass was found for a high-quality crystal.[13] Besides, a possible hidden magnetic order was suggested by anomalous Hall effect.[14] It appears that the magnetically critical behavior of the Pv $CaRuO_3$ is still highly underdebated.[15–21]

To solve the alleged contradictions, it could be helpful not only to study the Pv family $ARuO_3$ [A = Ca, Sr, Ba (Ref. 22)], but also to investigate related 4*d* oxides, such as $Sr_3Ru_2O_7$ (Ref. 23), $La_4Ru_6O_{19}$ (Ref. 24), Sr_2RuO_4 (Refs. 25 and 26), $SrRhO_3$ (Ref. 27), and $CaRhO_3$ (Refs. 28 and 29), which also demonstrate interesting electronic features. We think a magnetic study of the PPv $CaRuO_3$ can also help to address the issues regarding the magnetically critical behavior of the Pv $CaRuO_3$. Zhong *et al.*[30,31] have studied ground-state properties of the PPv $CaRuO_3$ from first-principles calculations within generalized gradient approximation (GGA) and GGA + U, which incorporates an additional on-site Coulomb interaction between 4*d* orbitals in Ru atoms. From these studies, they found that a metallic ferromagnetic state is stable within GGA, and the insulating antiferromagnetic (AFM) state becomes stable for GGA + U with $U \geqslant 2$ eV.

In this paper, we found a quasi-one-dimensional (1D) magnetism that is indicative of long-range AFM correlations in the PPv $CaRuO_3$. As a result, this is the observation of an integer ($S = 1$) AFM spin chain among 4*d*-correlated oxides.

II. EXPERIMENTAL METHODS

A polycrystalline-dense pellet (the observed density indicated <3% porosities) of the PPv $CaRuO_3$ was synthesized using a Kawai-type multi-anvil high-pressure apparatus at Gakushuin University.[1] First, we synthesized a precursor; mixed powder of $CaCO_3$ and RuO_2 was heated at 1150 °C for 14 h in air using a Pt crucible. The product was confirmed to be of the Pv $CaRuO_3$ by powder x-ray diffraction (XRD). Afterward, the powder was sealed in a Pt tube (1.5 mm in diameter and 5.7 mm in length). The tube was placed in the high-pressure apparatus with an MgO pressure medium and a $LaCrO_3$ thermal insulator; details of the high-pressure

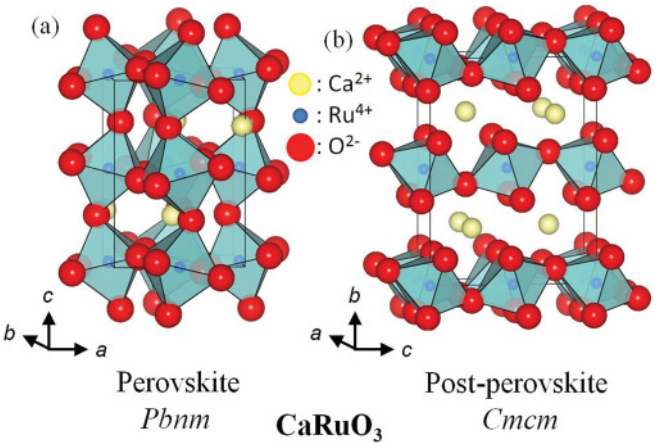

FIG. 1. (Color online) Sketch of the crystal structures of (a) the Pv and (b) the PPv $CaRuO_3$.[1] The figures used the same drawing scale. The PPv phase is 1.7% denser in volume than the Pv phase.[1] The crystal structures are drawn by using VESTA (Ref. 3).

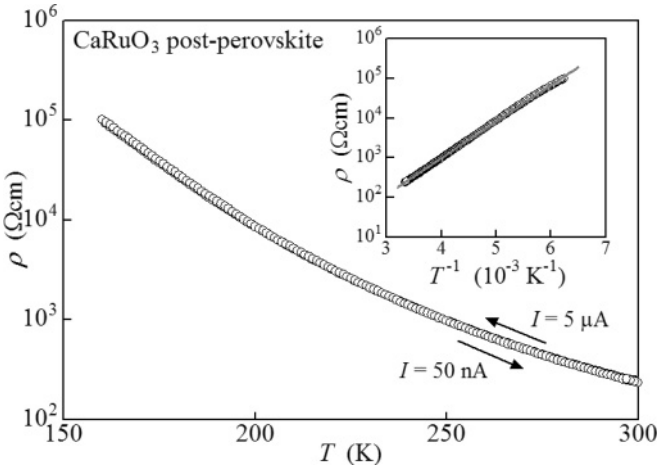

FIG. 2. T vs ρ of a polycrystalline and dense ($d_{obs}/d_{cal} > 0.97$) pellet of the PPv $CaRuO_3$. The inset shows the Arrhenius plot of the data.

cell were reported elsewhere.[1] Tungsten carbide anvils with truncated edge lengths of 2.5 mm were used. Temperature was measured by a Pt-Pt/13% Rh thermocouple. The synthesis temperature was between 1000 °C and 1040 °C, and the synthesis pressure was held constant at 23.5 GPa for a range between 1 and 5 h. The sample was quenched to room temperature within a few seconds before releasing the pressure. The recovered sample was confirmed to be of the PPv $CaRuO_3$ by XRD rather than the Pv $CaRuO_3$.[1]

Electrical resistivity (ρ) of the PPv $CaRuO_3$ was measured by a four-probe technique with a gauge current of 5 μA on cooling and 50 nA on warming. Electrical contacts on the four locations were made on the pellet by silver wires and paste. Magnetic susceptibility (χ) was measured in a fixed magnetic field of 1, 10, and 50 kOe in a commercial magnetometer [magnetic property measurement system (MPMS), Quantum Design, Inc.]. The polycrystalline sample was cooled to 2 K without applying the magnetic field and then was warmed to 300 K in the field [zero-field cooling, (ZFC)], followed by cooling [field cooling, (FC)]. The measurements were repeated in an oven in MPMS between 300 and 600 K as well. Isothermal magnetization was measured in MPMS at 10, 100, 200, 300, and 600 K between −70 and 70 kOe. The heat capacity at constant pressure (C_p) was measured in a commercial apparatus (physical property measurement system, Quantum Design, Inc.) by a quasiadiabatic method using the same pellet (13.61 mg) after the magnetic and electrical measurements were completed.

After the measurements above, the pellet was ground thoroughly and was mixed with an amount of Si powder at an approximate volume ratio of 1 to 1. The mixture was spread out evenly on a grease- coated glass plate (Apiezon N). The glass was mounted on a cold stage of a commercial XRD instrument (M03XHF22, Mac Science). Monochromatic radiation (Cu-Kα) was used in a 2θ range between 16° and 96°. The sample temperature was kept constant during the measurements ($|\Delta T| < 1$ K). At every temperature point, the sample position was properly adjusted to avoid a tiny mechanical shift due to the thermal effect of the cold stage. In addition, tabulated data of the thermal expansivity of Si were used to correct a 2θ shift.[32]

III. RESULTS AND DISCUSSION

Temperature effect on ρ of the PPv $CaRuO_3$ is shown in Fig. 2, which clearly indicates that the compound is semiconducting like over the whole temperature range. At low temperature, ρ goes beyond the technical limit. The curve's both cooling and warming follow the same trace exactly; indicating thermal hysteresis is not obvious over the temperature range. In order to further characterize the ρ feature, we analyzed the data by using the Arrhenius equation $\rho(T) = \rho_0 \exp(E_a/k_B T)$, where E_a, ρ_0, and k_B are an activation energy, a constant, and the Boltzmann constant, respectively. The theoretical curve fits the data as shown in the inset of Fig. 2 (solid line corresponds to the fitting) well, estimating E_a to be 0.18 eV.

Figure 3 shows temperature dependence of C_p for the PPv $CaRuO_3$. It is remarkable that a peak appears at 270 K, which is suggestive of a phase transition. To estimate the transition entropy ΔS, we first applied a polynomial function by a least-squares-linear method to the C_p data between 220 and 295 K except the transition part (see the solid curve in the main panel of Fig. 3). Then, we estimated ΔS to be 0.17 J mol^{-1} K^{-1}, as shown in the insets of Fig. 3. The ΔS is much smaller than the expected ΔS for the full order of the Ru^{4+} spins [$S = 1$; R ln 3 (∼9.13 J mol^{-1} K^{-1}), R is the ideal gas constant]; the observed ΔS corresponds to only 1.8% of the expectation. This suggests that much of the magnetic entropy is removed via short-range ordering (SRO) above the magnetic transition temperature if the peak is truly magnetic. Otherwise, a structure change on cooling is somewhat responsible for the observed ΔS. To test the possibility, we carefully conducted low-temperature XRD over the transition temperature.

Figure 4(a) shows all the XRD patterns in the order of temperature. The 300-K pattern was well characterized by the structure model (*Cmcm*) as performed in Ref. 1. We obtained the lattice parameters $a_0 = 3.114(1)$ Å, $b_0 = 9.826(1)$ Å, $c_0 = 7.297(1)$ Å, and $V_0 = 223.3(1)$ Å^3, by least-squares-

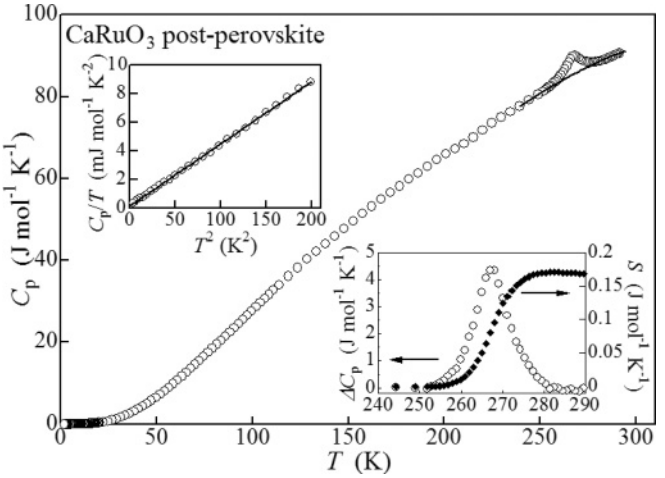

FIG. 3. (Main panel) C_p vs T and (upper inset) C_p/T vs T^2 of the PPv $CaRuO_3$.The lower inset shows an estimation of the transition entropy at ~270 K.

linear fitting to the peaks, to be identical with the reported values using CrKα radiation.[1] Upon cooling, evident changes, such as the appearance/disappearance of new peaks and the splitting of peaks were not detected, suggesting no symmetry change on the lattice. Figure 4(b) shows the temperature dependence of the orthorhombic lattice parameters deduced from the XRD analysis. The lattice parameters anisotropically change on cooling; b and c gradually decrease, while a slightly increases. The anisotropic change is obvious; however, the unit-cell volume monotonically decreases without any anomalies. The decrease in volume with temperature is comparable with that of the Pv $CaRuO_3$ [dotted curve in Fig. 4(b) (Ref. 33)]. Over the XRD measurements, we found that a structure change is unlikely coupled with the C_p peak at 270 K.

In the low-temperature limit of C_p/T vs T^2 (upper inset of Fig. 3), we applied the approximated Debye function $C_v/T = \gamma + \beta T^2$ ($T \ll \Theta_D$) to analyze the part, where C_v, γ, β, and Θ_D are heat capacity at constant volume, the Sommerfeld coefficient, a coefficient, and the Debye temperature, respectively. By the fitting, we estimated γ to be 0.16(2) mJ mol^{-1} K^{-2} and $\beta = 4.34(2) \times 10^{-5}$ J mol^{-1} K^{-4}. Θ_D was calculated to be 607(3) K from β. The value of γ is fairly smaller than that of the Pv $CaRuO_3$ [73 mJ mol^{-1} K^{-2} (Ref. 19)], being qualitatively consistent with the observed semiconducting nature; conducting carriers in the PPv $CaRuO_3$ are too few to establish a metallic conduction. The observed Θ_D is slightly higher than the value 495 K found for the Pv $CaRuO_3$.[8] It should be noted that a comparable increase in the Debye temperature by the PPv transition was found for $CaRhO_3$,[29] while it was not for $MgSiO_3$ (Ref. 34).

Figure 5 shows temperature dependence of χ of the PPv $CaRuO_3$ measured in a magnetic field of 50 kOe. The curve shows a wide hump with the maximum at 470 K, suggesting a quasi-1D magnetism.[35] In addition, a small kink was found at ~270 K (see the differential curve shown at the bottom of Fig. 5), which is presumably coupled with the C_p peak. To analyze the possible quasi-1D magnetism, we applied the

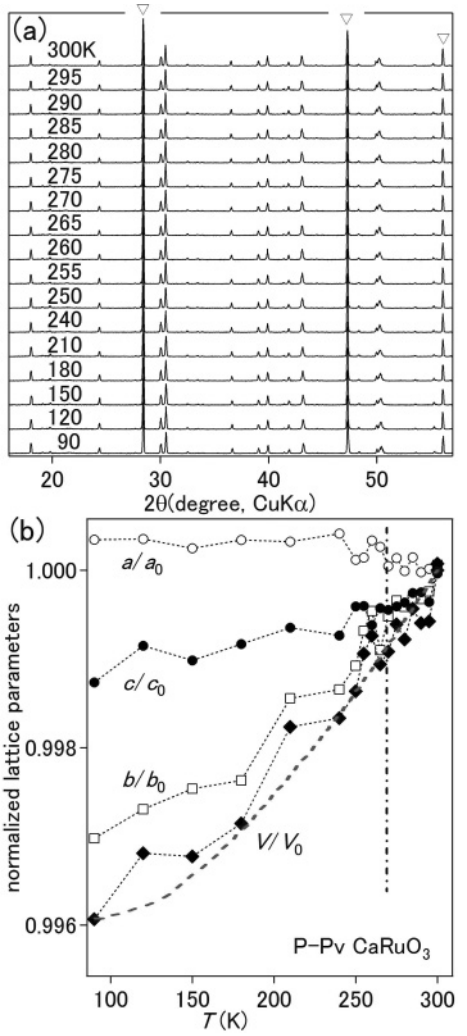

FIG. 4. (Color online) (a) Low-temperature XRD patterns and (b) temperature dependence of the normalized lattice parameters of the PPv $CaRuO_3$ (*Cmcm*). The 300-K parameters $a_0 = 3.115(1)$ Å, $b_0 = 9.826(1)$ Å, $c_0 = 7.297(1)$ Å, and $V_0 = 223.3(1)$ Å^3 were used in the plot. The open triangles correspond to Si peaks. The broken line corresponds to the magnetic ordering temperature of the PPv $CaRuO_3$, and the fat dotted curve indicates the V/V_0 curve for the Pv $CaRuO_3$ (taken from Ref. 33).

following equation to the experimental curve, which is valid for a 1D AFM Heisenberg spin chain with $S = 1$ (Ref. 36):

$$\chi_{calc} = \frac{N_A \mu_B^2 g^2}{k_B T}\left(\frac{2 + 0.0194X + 0.777X^2}{3 + 4.346X + 3.232X^2 + 5.834X^3}\right) + \chi_0 \quad \text{and} \quad X \equiv \frac{|J|}{k_B T},$$

where, N_A, μ_B, g, J, and χ_0 are the Avogadro number, the Bohr magneton, Landé's general factor, the exchange energy, and a T-independent term, respectively. At $\chi_0 = 0$, the agreement factor, $[\sum(\chi_{obs} - \chi_{calc})^2 / \sum \chi_{obs}^2]^{1/2}$, decreases to 0.001 03 over the temperature range from 400 to 600 K, indicating a good fit. In the analysis, the magnetic parameters $-J/k_B$ and g were estimated to be 350 K ($|J| = 30.2$ meV) and 2.053, respectively. At $\chi_0 \neq 0$, $-J/k_B$, χ_0, and the agreement factor were estimated to be 350 K, 3.99×10^{-5} emu/mol, and 0.000 98,

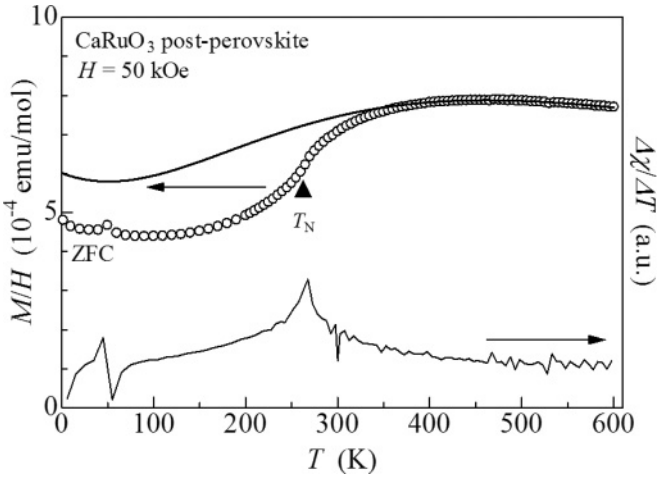

FIG. 5. T dependence of the magnetic susceptibility of the PPv $CaRuO_3$ measured at 50 kOe and a (solid curve) theoretical curve fitting to the data. Differential curve at the bottom indicates an anomaly at ~270 K. (a.u. means arb. units.)

respectively (g was fixed at 2), indicating there is no significant difference between the magnetic parameters with and without χ_0.

The excellent agreement between the experimental and theoretical curves implies that the 1D AFM magnetism is likely above 270 K. It is possible that a 1D spin chain is formed along the a axis via the Ru-O-Ru bond that has significant π-type interorbital interactions; we will discuss this later. However, disagreement between the theoretical and experimental curves in T vs χ is obvious below approximately 350 K. Considering the absence of the structure anomaly and the ρ-T anomaly in the vicinity of 270 K, the disagreement is likely due to the establishment of an AFM order in the long range. If this is true, T_N is 270 K, which is three times higher than T_N of the PPv $CaRhO_3$ (Ref. 29).

In Fig. 6, temperature dependence of χ of the PPv $CaRuO_3$ measured in a weaker magnetic field of 1 kOe is shown. The magnetic anomaly at ~270 K is very obvious. In addition, another anomaly at ~90 K appears with remarkable thermal

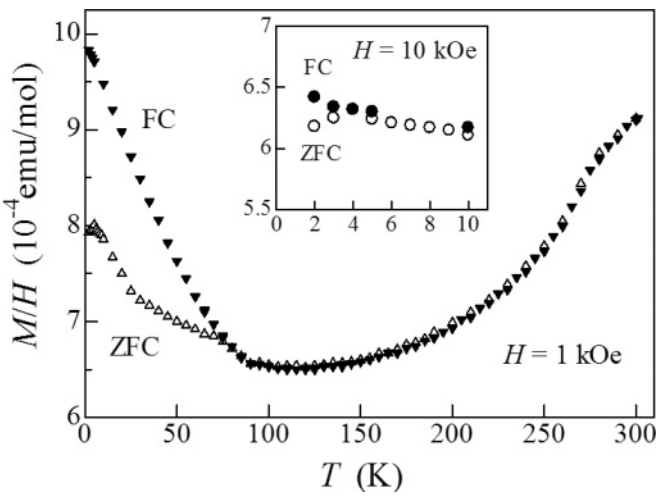

FIG. 6. Thermal hysteresis of the magnetic susceptibility of the PPv $CaRuO_3$ measured at (main panel) 1 kOe and (inset) 10 kOe.

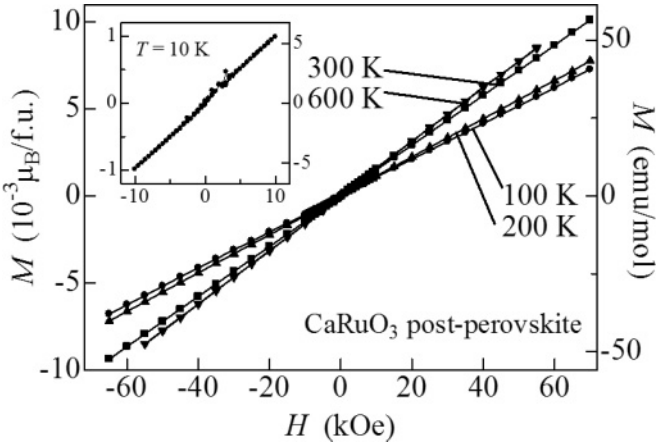

FIG. 7. Isothermal magnetization at various temperatures of the polycrystalline PPv $CaRuO_3$. (f.u. stands for formula units.) The inset shows the data measured at 10 K.

hysteresis between the FC and the ZFC curves. Furthermore, an additional small peak can be seen at ~4 K, which is confirmed in a 10-kOe measurement (inset in Fig. 6). These multiple anomalies appear only in weaker fields, and those are reminiscent of what was observed for the Pv $CaRuO_3$, for which a spin-glass-like order was suggested.[13] Uniaxial strain in the crystal possibly accounts for the magnetically glassy behaviors, as discussed in Refs. 37 and 38. If this is true, we may expect a similar mechanism for the PPv $CaRuO_3$. Alternatively, it is possible that undetected magnetic impurities are responsible for the anomalies to some extent, such as a possible intermediate phase between the Pv and the PPv as recently found in the Ca-Rh-O system.[39]

To characterize the magnetic properties further, we measured isothermal magnetization at various temperatures in a wide temperature range; the data are presented in Fig. 7. We observed only linear features regardless of the magnetic transition at 270 K. This directly indicates that the PPv $CaRuO_3$ does not include ferromagnetic interactions in the magnetic system unlike the Pv $CaRuO_3$. Thus, it is interesting to search for a ferromagnetic interaction possibly hidden in the PPv $CaRuO_3$ by introducing disorders as performed for the Pv $CaRuO_3$ (Refs. 11 and 12); the study is in progress.

Here, we compare the magnetic properties of the PPv $CaRuO_3$ (Ru^{4+}:$4d^4$) with those of the analogous oxides $CaIrO_3$ (Ir^{4+}:$5d^5$) (Refs. 40and 41), $NaIrO_3$ (Ir^{5+}:$5d^4$) (Ref. 42), and $CaRhO_3$ (Rh^{4+}:$4d^5$) (Refs. 28 and 29). Numerical comparison is provided in Table I. We actually investigated five PPv oxides synthesized so far, $CaRuO_3$, $CaRhO_3$, $NaIrO_3$, $CaIrO_3$, and $CaPtO_3$; however, $CaPtO_3$ was confirmed not to be magnetically active, as was expected (Pt^{4+}:$5d^6$, t_{2g}^6, $S = 0$) (Refs. 43 and 44). Thus, we excluded $CaPtO_3$ from the comparison.

Unlike $CaRuO_3$, the PPvs $CaIrO_3$ and $CaRhO_3$ show Curie-Weiss (CW) paramagnetism (CWP). Because each compound has a well-localized electronic state, the CW parameters (the Weiss temperature Θ_W and the effective magnetic moment μ_{eff}) can be good indicators of the magnetic state; the CW parameters suggest that AFM interactions play a dominant role

TABLE I. Comparison of the magnetic parameters of the post-perovskite $CaRuO_3$ with those of the related post-perovskite and perovskite oxides.

Compounds		S	Θ_W (K)	μ_{eff} (μ_B)	M_0 (μ_B)[a]	T_N (K)	Magnetic feature[b]	E_a (eV)[c]	References
Post-perovskite type structure									
$CaRuO_3$	Ru^{4+}: $4d^4$ (t_{2g}^4)	1	–	–	–	270	AFM	0.18	This work
$CaRhO_3$	Rh^{4+}: $4d^5$ (t_{2g}^5)	1/2	−1071	2.99	0.03	90	CAFM	0.038	29
$NaIrO_3$	Ir^{5+}: $5d^4$ (t_{2g}^4)	1	−2.2	0.28	–	–	CWP	VRH	42
$CaIrO_3$	Ir^{4+}: $5d^5$ (t_{2g}^5)	1/2	−1800	3.29	0.037	115	CAFM	0.17	40
$CaPtO_3$	Pt^{4+}: $5d^6$ (t_{2g}^6)	0	–	–	–	–	D	–	43,44
Perovskite type structure									
$CaRuO_3$	Ru^{4+}: $4d^4$ (t_{2g}^4)	1	−68	2.2	–	–	CWP	Metallic	19
$CaRhO_3$	Rh^{4+}: $4d^5$ (t_{2g}^5)	1/2	−650	3.52	–	–	CWP	Metallic	28,29
$CaIrO_3$	Ir^{4+}: $5d^5$ (t_{2g}^5)	1/2	–	–	–	–	PP	Metallic	40

[a] M_0: spontaneous magnetization.
[b] (CAFM) canted AFM, (PP) Pauli paramagnetism, (D) diamagnetism.
[c] E_a: activation energy measured in electrical transport measurement. (VRH) variable range hopping conduction.

between spins. The AFM interactions reasonably account for the AFM long-range order observed for $CaIrO_3$ ($T_N = 115$ K) and $CaRhO_3$ (90 K). Meanwhile, a relatively small degree of the transition entropy at T_N (4.4% of the full spin order ΔS for $CaRhO_3$) suggests that an AFM SRO is significant above T_N (Ref. 29). $NaIrO_3$ also was reported to show CW features without long-range AFM order (no evidence of magnetic order at 2 K), however, it was argued that a small amount of magnetic impurities may be responsible for the feature.[42] As a result of the comparison, it becomes clear that the PPv $CaRuO_3$ shows a distinct magnetism.

The microscopic origin of the quasi-1D magnetism of the PPv $CaRuO_3$ may be discussed better after additional studies by microscopic probes, such as NMR and μSR are completed; nevertheless, consideration of the electronic configuration and the structure can reasonably provide a microscopic picture of the quasi-1D magnetism. Looking at the Ru-O bond in the RuO_6 octahedra, four bonds are 2.039(2) Å, and two bonds are 1.947(2) Å, indicating a 4.7% in difference.[1] Thus, it can be expected that the axial compression along the z direction, which is defined as parallel to the Ru-O1 bond in each RuO_6 octahedron,[1] should render the $4d_{xy}$ level lower in energy than the $4d_{yz}$ and $4d_{zx}$ levels (the $4d_{yz}$ and $4d_{zx}$ orbitals are nearly degenerate). Therefore, it is reasonably expected that the magnetic ground state is $S = 1$ ($4d_{xy}^2 4d_{yz}^1 4d_{zx}^1$) for the PPv $CaRuO_3$.

To verify these qualitative arguments, we examined electronic structures of the PPv $CaRuO_3$ from first-principles calculations within density functional theory. The full-potential augmented plane-wave method was employed with the WIEN2k package.[45] The exchange-correlation energy is treated by GGA with the Perdew-Burke-Ernzerhof functional.[46] In Fig. 8(a), we show total density of states and partial densities of states (PDOS) for non-spin-polarized calculations. From the PDOS decomposed for individual d orbitals in a Ru atom, we clearly see that Ru $4d$ bands split into the empty e_g ($3z^2 - 1, x^2 - y^2$) and the partially filled t_{2g} (xy, yz, zx) bands. In addition, the PDOS of d_{xy} distributes at lower energy than those of d_{yz} and d_{zx}. Such splitting is caused by the aforementioned distortion of the RuO_6 octahedra. Hence, the Ru $4d$ configuration can be described as $S = 1$ ($4d_{xy}^2 4d_{yz}^1 4d_{zx}^1$).

When magnetic orderings are included in first-principles calculations, the state with magnetic moments aligned AFM along the a and c axes was found to be more stable than the non-spin-polarized and the ferromagnetic states by 8 and 4 meV per Ru atom, respectively. For this AFM alignment, we must construct a supercell that is doubled along the a axis. This state has not been taken into account in the previous studies, while several other magnetic orderings have been discussed.[30,31] From the PDOS shown in Fig. 8(b), we found that the magnetic moments arise from the exchange splittings of d_{yz} and d_{zx} levels, and both majority and minority spin bands of d_{xy} are occupied. Thus, the distribution of PDOS indicates that Ru $4d$ is indeed in the low spin $S = 1$ configuration. We should note, however, that the calculated AFM states fail to reproduce the experimentally observed insulating behavior. The system is calculated as metallic, although the Fermi energy is located in a pseudogap caused by magnetic ordering. Such disagreement is well known as a failure of GGA. When the on-site Coulomb interaction was included as an additional term in GGA + U, the AFM phase became insulating for $U \sim 1$ eV without changing the splitting between d levels. Detailed results with GGA + U will be reported elsewhere.

The studies above suggest that the magnetic infinite chain is formed along the a axis by sharing the common edges of RuO_6 octahedra. The nearly equivalent superexchange paths d_{yz}-$2p_\pi$-d_{zx} and d_{zx} -$2p_\pi$-d_{yz} connect the neighbor RuO_6 octahedra magnetically more strongly along the a axis than the other directions, resulting in the magnetic anisotropy toward 1D. The magnetic bond along the c axis is mainly responsible for the Ru-O-Ru bond with 139°, which is through the corner-shared RuO_6 octahedra.[1] The neighbor Ru-Ru distance is 18% longer along the c axis than that along the a axis.[1] Thus, the c-axis magnetic path can be expected to be not as strong, rejecting the possibility of an in-plane two-dimensional magnetism. Meanwhile, it is reasonable to expect that the t_{2g}^5 compounds, such as $CaRhO_3$ and $CaIrO_3$ do not form a comparable magnetic path because one of the d_{zx} or d_{yz} orbitals is filled by paired $4d$ electrons. The d_{zx} and d_{yz} are almost energetically degenerate; thus, freedom kills any long-range AFM correlation.[47,48] This fundamentally accounts for the

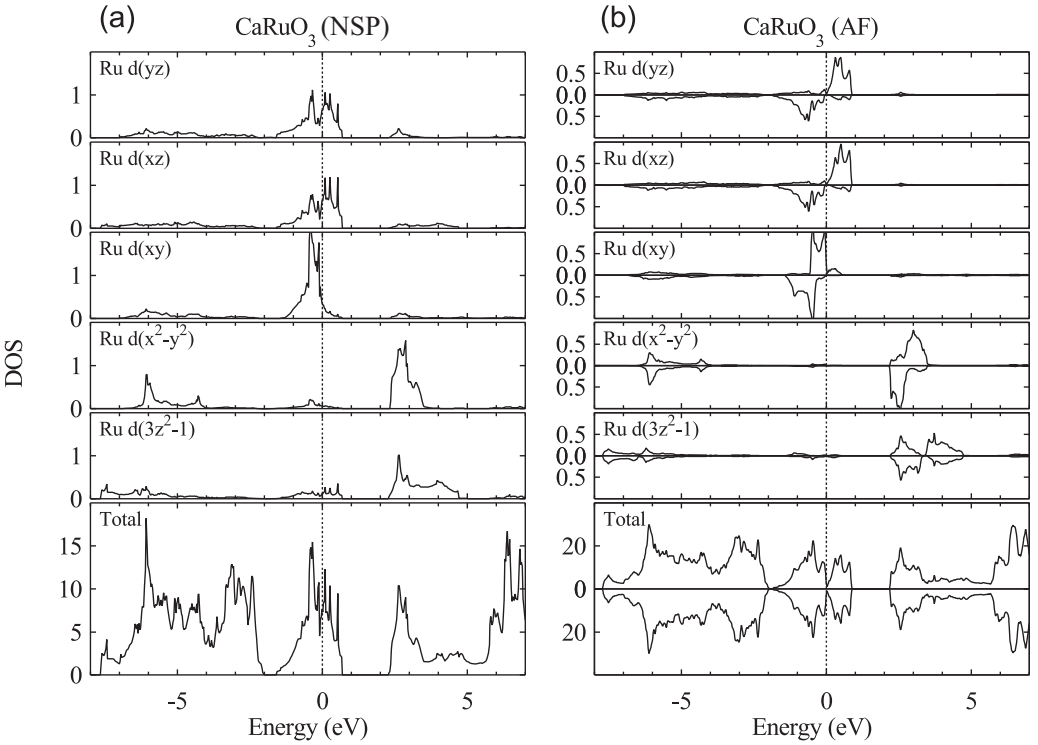

FIG. 8. Total density of states and PDOS for the PPv $CaRuO_3$. We use a local coordinate system, which has a z axis along the Ru-O1 bond and the x axis approximately along the Ru-O2 bond. (a) Non-spin-polarized states, (b) AFM states.

absence of the quasi-1D magnetism in the t_{2g}^5 compounds $CaIrO_3$ and $CaRhO_3$.

Here, we should state our general picture for the magnetic interactions of the PPv compounds: (1) quasi-1D AFM correlations are formed along the edge-shared octahedral direction (a axis), (2) freedom of the twofold degenerate d_{zx} and d_{yz} orbitals plays the predominant role of establishment of the long-rang magnetic order, and (3) minor AFM interactions work along the corner-shared octahedral direction (c axis).

In conclusion, we found the PPv $CaRuO_3$ showed a quasi-1D magnetism owing to the superexchange magnetic paths d_{yz}-$2p_\pi$-d_{zx} and d_{zx}-$2p_\pi$-d_{yz} along the a axis. As a result, this is an example of integer spin-chain magnetism for a $4d$ electron system. A half-integer ($S = 1/2$) spin chain was recently discovered for the $4d$ compound $AgSO_4$ (Ref. 49) in which extended superexchange interactions[50] via (Ag^{2+}-O)-(O-Ag^{2+}) with $-J/k_B = 217$ K play a dominant role to form a Heisenberg AFM chain. Because the magnetic ground states of integer and half-integer AFM spin chains are entirely different,[51–53] further studies of both $4d$ compounds can help to understand the underlying physics of $4d$ spin chain.

The AFM correlation of $CaRuO_3$ is much stronger ($-J/k_B = 350$ K) than that of $AgSO_4$. Thus, it is of great interest to investigate new magnetic properties that may arise from carrier doping of this novel $4d$ system. We are actively pursuing high-pressure experiments to establish the reaction conditions that will result in doping. Besides, the PPv $CaRuO_3$ is unique in that it is isocompositional but not isostructural with the Pv $CaRuO_3$. Further study of the PPv $CaRuO_3$ can help to define the fundamental nature of magnetism in the ruthenate family.

ACKNOWLEDGMENTS

We thank Dr. K. Ohgushi (University of Tokyo), Dr. Y. Tsujimoto (NIMS), and Dr. J. S. Zhou (University of Texas) for discussions. This research was supported in part by the WPI Initiative on Materials Nanoarchitectonics from the Ministry of Education, Culture, Sports, Science and Technology, Japan; Research Seeds Quest Program, managed by the Japan Science and Technology Agency; and Grants-in-Aid for Scientific Research (Grants No. 20360012, No. 22246083, No. 22340163, No. 21360325, No. 20110002, and No. 21540497) and the Funding Program for World-Leading Innovative R and D on Science and Technology (FIRST Program), managed by the Japan Society for the Promotion of Science.

*09242001@gakushuin.ac.jp (Y. Shirako)

[1]H. Kojitani, Y. Shirako, and M. Akaogi, Phys. Earth Planet. Inter. **165**, 127 (2007).

[2]Y. Shirako, H. Satsukawa, H. Kojitani, T. Katsumata, M. Yoshida, Y. Inaguma, K. Hiraki, T. Takahashi, K. Yamaura, E. Takayama-Muromachi, and M. Akaogi, J. Phys.: Conf. Ser. **215**, 012038 (2010).

[3]K. Momma and F. Izumi, J. Appl. Crystallogr. **41**, 653 (2008).

[4]T. C. Gibb, R. Greatrex, N. N. Greenwood, and P. Kaspi, J. Chem. Soc. Dalton Trans. **12**, 1253 (1973).

[5]M. Shepard, G. Cao, S. McCall, F. Freibert, and J. E. Crow, J. Appl. Phys. **79**, 4821 (1996).
[6]J. M. Longo, P. M. Raccah, and J. B. Goodenough, J. Appl. Phys. **39**, 1327 (1968).
[7]K. Yoshimura, T. Imai, T. Kiyama, K. R. Thurber, A. W. Hunt, and K. Kosuge, Phys. Rev. Lett. **83**, 4397 (1999).
[8]T. Kiyama, K. Yoshimura, K. Kosuge, H. Michor, and G. Hilscher, J. Phys. Soc. Jpn. **67**, 307 (1998).
[9]T. Kiyama, K. Yoshimura, and K. Kosuge, J. Phys. Soc. Jpn. **68**, 3372 (1999).
[10]H. Mukuda, K. Ishida, Y. Kitaoka, K. Asayama, R. Kanno, and M. Takano, Phys. Rev. B **60**, 12279 (1999).
[11]T. He and R. J. Cava, Phys. Rev. B **63**, 172403 (2001).
[12]T. He and R. J. Cava, J. Phys.: Condens. Matter **13**, 8347 (2001).
[13]I. Felner, I. Nowik, I. Bradaric, and M. Gospodinov, Phys. Rev. B **62**, 11332 (2000).
[14]P. Khalifah, I. Ohkubo, B. C. Sales, H. M. Christen, D. Mandrus, and J. Cerne, Phys. Rev. B **76**, 054404 (2007).
[15]S. C. Gausepohl, M. Lee, R. A. Rao, and C. B. Eom, Phys. Rev. B **54**, 8996 (1996).
[16]A. Koriyama, M. Ishizaki, T. C. Ozawa, T. Taniguchi, Y. Nagata, H. Samata, Y. Kobayashi, and Y. Noro, J. Alloys Compd. **372**, 58 (2004).
[17]J. S. Lee, Y. S. Lee, T. W. Noh, S. Nakatsuji, H. Fukazawa, R. S. Perry, Y. Maeno, Y. Yoshida, S. I. Ikeda, J. Yu, and C. B. Eom, Phys. Rev. B **70**, 085103 (2004).
[18]K. Maiti and R. S. Singh, Phys. Rev. B **71**, 161102(R) (2005).
[19]G. Cao, S. McCall, M. Shepard, J. E. Crow, and R. P. Guertin, Phys. Rev. B **56**, 321 (1997).
[20]G. Cao, O. Korneta, S. Chikara, L. E. DeLong, and P. Schlottmann, Solid State Commun. **148**, 305 (2008).
[21]H. Kawanaka, M. Yokoyama, A. Noguchi, H. Bando, and Y. Nishihara, J. Phys.: Condens. Matter **21**, 296002 (2009).
[22]C.-Q. Jin, J.-S. Zhou, J. B. Goodenough, Q. Q. Liu, J. G. Zhao, L. X. Yang, Y. Yu, R. C. Yu, T. Katsura, A. Shatskiy, and E. Ito, Proc. Natl. Acad. Sci. USA **107**, 14026 (2010).
[23]S. A. Grigera, R. S. Perry, A. J. Schofield, M. Chiao, S. R. Julian, G. G. Lonzarich, S. I. Ikeda, Y. Maeno, A. J. Millis, and A. P. Mackenzie, Science **294**, 329 (2001).
[24]P. Khalifah, K. D. Nelson, R. Jin, Z. Q. Mao, Y. Liu, Q. Huang, X. P. Gao, A. P. Ramirez, and R. J. Cava, Nature (London) **411**, 669 (2001).
[25]Y. Maeno, H. Hashimoto, K. Yoshida, S. Nishizaki, T. Fujita, J. G. Bednorz, and F. Lichtenberg, Nature (London) **372**, 532 (1994).
[26]E. V. Kuz'min and S. G. Ovchinnikov, Phys. Solid State **41**, 1775 (1999).
[27]K. Yamaura and E. Takayama-Muromachi, Phys. Rev. B **64,** 224424 (2001).
[28]K. Yamaura and E. Takayama-Muromachi, Physica C **445-448**, 54 (2006).
[29]K. Yamaura, Y. Shirako, H. Kojitani, M. Arai, D. P. Young, M. Akaogi, M. Nakashima, T. Katsumata, Y. Inaguma, and E. Takayama-Muromachi, J. Am. Chem. Soc. **131**, 2722 (2009).
[30]G. H. Zhong, Y. L. Li, Z. Liu, and H. Q. Lin, J. Appl. Phys. **107**, 09E102 (2010).
[31]G. H. Zhong, Y. L. Li, Z. Liu, and Z. Zeng, Solid State Sci. **12**, 2003 (2010).
[32]D. N. Batchelder and R. O. Simmonss, J. Chem. Phys. **41**, 2324 (1964).
[33]T. Kiyama, K. Yoshimura, K. Kosuge, Y. Ikeda, and Y. Bando, Phys. Rev. B **54**, R756 (1996).
[34]M. Akaogi and E. Ito, Geophys. Res. Lett. **20**, 105 (1993).
[35]J. C. Bonner and M. E. Fisher, Phys. Rev. **135**, A640 (1964).
[36]A. Meyer, A. Gleizes, J. J. Girerd, M. Verdaguer, and O. Kahn, Inorg. Chem. **21**, 1729 (1982).
[37]A. T. Zayak, X. Huang, J. B. Neaton, and Karin M. Rabe, Phys. Rev. B **77**, 214410 (2008).
[38]M. Schultz, L. Klein, J. W. Reiner, and M. R. Beasley, Phys. Rev. B **73**, 085109 (2006).
[39]M. Akaogi, Y. Shirako, H. Kojitani, S. Takamori, K. Yamaura, and E. Takayama-Muromachi, J. Phys.: Conf. Ser. **215**, 012095 (2010).
[40]K. Ohgushi, H. Gotou, T. Yagi, Y. Kiuchi, F. Sakai, and Y. Ueda, Phys. Rev. B **74**, 241104 (2006).
[41]R. F. Sarkozy, C. W. Moeller, and B. L. Chamberland, J. Solid State Chem. **9**, 242 (1974).
[42]M. Bremholm, S. E. Dutton, P. W. Stephens, and R. J. Cava, J. Solid State Chem. **184**, 601 (2011).
[43]K. Ohgushi, Y. Matsushita, N. Miyajima, Y. Katsuya, M. Tanaka, F. Izumi, H. Gotou, Y. Ueda, and T. Yagi, Phys. Chem. Miner. **35**, 189 (2008).
[44]Y. Inaguma, K. Hasumi, M. Yoshida, T. Ohba, and T. Katsumata, Inorg. Chem. **47**, 1868 (2008).
[45]P. Blaha, K. Schwarz, G. K. H. Madsen, D. Kvasnicka, and J. Luitz, *WIEN2k, An Augmented Plane Wave + Local Orbitals Program for Calculating Crystal Properties* (Karlheinz Schwarz, Technische Universität Wien, Austria, 2001).
[46]J. P. Perdew, K. Burke, and M. Ernzerhof, Phys. Rev. Lett. **77**, 3865 (1996).
[47]J. B. Goodenough and J. S. Zhou, Chem. Mater. **10**, 2980 (1998).
[48]Y. Tokura and N. Nagaosa, Science **288**, 462 (2000).
[49]P. J. Malinowski, M. Derzsi, Z. Mazej, Z. Jagličić, B. Gaweł, W. Łasocha, and W. Grochala, Angew. Chem., Int. Ed. **49**, 1683 (2010).
[50]Y. G. Shi, Y. F. Guo, S. Yu, M. Arai, A. Sato, A. A. Belik, K. Yamaura, and E. Takayama-Muromachi, J. Am. Chem. Soc. **132**, 8474 (2010).
[51]T. Giamarchi, *Quantum Physics in One Dimension* (Clarendon, Oxford, 2003).
[52]F. D. M. Haldane, Phys. Rev. Lett. **50**, 1153 (1983).
[53]I. Affleck, T. Kennedy, E. H. Lieb and H. Tasaki, Phys. Rev. Lett. **59**, 799 (1987).